Frontiers in Bioscience Landmark

Front. Biosci. (Landmark Ed) **2026**; 31(9): 54612
https://doi.org/10.31083/FBL54612

Original Research

TMEM61 Promotes Malignant Behaviors and Maintains Genomic Stability in Ovarian Cancer Cells

Zhizheng Dai[1,†], Ruilian Tong[1,†], Kai-Fu Tang[1,*]

[1]Key Laboratory of Molecular Biology on Infectious Diseases, Ministry of Education, Chongqing Medical University, 400010 Chongqing, China
*Correspondence: tangkaifu@cqmu.edu.cn (Kai-Fu Tang)
[†]These authors contributed equally.

Academic Editor: Sung Eun Kim
Submitted: 5 June 2026 Revised: 30 July 2026 Accepted: 10 August 2026 Published: 15 September 2026

Abstract

Background: Transmembrane protein 61 (TMEM61) has previously been reported in several malignancies. However, its function in ovarian cancer remains unclear. Here, we aimed to investigate the role and underlying mechanisms of TMEM61 in ovarian cancer cells. **Methods:** Differentially expressed genes were identified by analyzing transcriptomic data of 426 ovarian cancer tissues from The Cancer Genome Atlas database and 88 normal ovarian tissues from the Genotype-Tissue Expression database using the web-based analytical tool GEPIA2. The effects of TMEM61 knockdown on ovarian cancer cell invasion, migration, and proliferation were evaluated using Transwell, wound healing, and Cell Counting Kit-8 assays. The effect of TMEM61 knockdown on DNA damage and cytosolic DNA accumulation was assessed using immunofluorescence and comet assays. TMEM61 and programmed death-ligand 1 (PD-L1) expression levels were assessed using immunoblotting and reverse transcription-quantitative polymerase chain reaction. **Results:** TMEM61 exhibited very low expression in normal ovarian tissues, but its expression was significantly upregulated in ovarian cancer tissues. TMEM61 knockdown significantly inhibited the proliferation, migration, and invasion of ovarian cancer cells; induced DNA damage and cytoplasmic DNA accumulation; and upregulated PD-L1 expression in ovarian cancer cells. **Conclusions:** TMEM61 promotes malignant behavior and maintains genomic stability in ovarian cancer cells. TMEM61 may serve as a potential biomarker and molecular target for ovarian cancer.

Keywords: ovarian cancer cells; transmembrane protein 61; cell proliferation; cell migration and invasion; DNA damage; programmed death-ligand 1

1. Introduction

Ovarian cancer is one of the most devastating gynecological malignancies and creates a substantial health burden for women globally. Owing to non-specific early clinical manifestations and the unavailability of effective population-level screening modalities, the majority of cases are diagnosed at advanced disease stages. Despite standard-of-care cytoreductive surgery followed by chemotherapy, clinical benefits remain limited, with tumor recurrence and distant metastasis occurring in a substantial proportion of patients [1,2,3].

Major advances have been made in the development of targeted therapies and immunotherapies for ovarian cancer management [1,3,4,5,6]. Targeted therapies interfere with specific oncogenic signaling cascades to suppress tumor growth and progression. By contrast, cancer immunotherapy mediates tumor elimination by harnessing endogenous immune circuits. In ovarian cancer, immunotherapeutic interventions can trigger and amplify anti-tumor immune responses to eliminate malignant cells [4,5]. Immune checkpoint-blockade therapeutics represent one of the major cornerstones of current-day cancer immunotherapy. Therapeutic antibodies that disrupt the programmed cell death protein 1 (PD-1)/Programmed death-ligand 1 (PD-L1) axis represent the most prevalently deployed clinical tools in this category [7,8]. PD-1, a co-inhibitory receptor expressed primarily on T lymphocytes, receives suppressive signals upon binding to its ligand PD-L1, which is detectable on both antigen-presenting cells and malignant tumor cells. This receptor–ligand interaction dampens T-cell activation and clonal expansion [7,9]. Many tumor types upregulate the expression of PD-L1, which engages T-cell PD-1 to abrogate cytotoxic antitumor responses and enable tumor immune evasion. Therapeutic monoclonal antibodies targeting PD-1 or PD-L1 can disrupt this inhibitory interaction. Blocking PD-L1-PD-1 engagement reinstates the antitumor effector capacity of T lymphocytes [7,10].

Although targeted therapies and immunotherapies for ovarian cancer have demonstrated promising effects, several challenges remain. These include the need to improve treatment efficacy and specificity, minimize toxicity and adverse effects, and enhance the prediction of therapeutic outcomes [1,4,5,11,12]. To address these challenges, we screened genes specifically expressed in ovarian cancer cells and identified transmembrane protein 61 (TMEM61) as a candidate for further examination. Transmembrane proteins constitute a large protein family predominantly residing in the plasma membrane and intracellular organelle

membranes. Growing evidence indicates that TMEM proteins drive oncogenesis and cancer progression by regulating fundamental cellular processes, including cell proliferation, cellular differentiation, apoptotic responses, signaling cascades, and molecular trafficking [13,14,15,16]. However, the role of TMEM61 in the development and progression of ovarian cancer remains unclear. Therefore, in this study, we aimed to investigate the role of TMEM61 and its underlying mechanism in ovarian cancer cells.

2. Materials and Methods

2.1 Cell Culture

T29H cells were provided by Professor Jin Song Liu from the University of Texas MD Anderson Cancer Center [17] and cultured in Dulbecco's Modified Eagle's medium (KeyGEN BioTECH, Nanjing, China) containing 10% fetal bovine serum (FBS; BasalMedia Technologies Co., Ltd., Shanghai, China) and 1% penicillin–streptomycin. SKOV3 cells (from The American Type Culture Collection, Manassas, VA, USA) were maintained in Roswell Park Memorial Institute 1640 medium (KeyGEN BioTECH) containing 10% FBS and 1% penicillin–streptomycin. All the cell cultures were maintained at 37 °C in a humidified atmosphere containing 5% CO_2. Mycoplasma screening assays were performed to verify the absence of mycoplasma-derived contaminants. Cells cultured in the laboratory for more than six months post-receipt were genotyped using polymorphic short tandem repeat loci.

2.2 DNA and siRNA Transfection

The siRNAs were synthesized by GenePharma Co., Ltd. (Shanghai, China). The following siRNAs were used in the current study: siTMEM61-1: 5′-GCCUGCUGUGGUCCGUCAA-3′, 5′-UUGACGGACCACAGCAGGC-3′; siTMEM61-2: 5′-CGUUUCUGCGGAGACGACA-3′, 5′-UGUCGUCUCCGCAGAAACG-3′; siNC: 5′-AAUUCUCCGAACGUGUCACGUTT-3′, 5′-ACGUGACACGUUCGGAGAAUUTT-3′. The plasmids used in this study included: pTREX1 (Addgene, Cambridge, MA, USA), pCBASceI (Addgene), pSceI-Hygro-EGFP (Custom-made by Yingmaoshengye Biotechnology, Beijing, China), and pDR-GFP (Addgene). Plasmid constructs and siRNAs were delivered into T29H and SKOV3 cell lines using Lipofectamine 2000 transfection reagent (Thermo Fisher Scientific, Waltham, MA, USA).

2.3 Immunoblotting

Cells were lysed at 4 °C using RIPA buffer containing a protease inhibitor cocktail (APExBIO, Houston, TX, USA). Equal amounts of cell lysate were separated via sodium dodecyl sulfate-polyacrylamide gel electrophoresis (SDS-PAGE), and the proteins were electrotransferred onto polyvinylidene fluoride (PVDF) membranes (EMD Millipore, Danvers, MA, USA). After blocking non-specific binding, the membranes were incubated overnight at 4 °C with the primary antibodies, including anti-TMEM61 (Immunoway, San Jose, CA, USA; Cat#YN7530; 1:1000), anti-Flag (HUABIO, Hangzhou, Zhejiang, China; Cat#0912-1; 1:5000), anti-PD-L1 (Abcam, Cambridge, Cambridgeshire, UK; ab205921; 1:1000), and anti-GAPDH (Proteintech, Wuhan, Hubei, China; 60004-1-AP; 1:1000). Membranes were then incubated with an HRP-conjugated secondary antibody for 1 h at 24 °C. Immunoreactive bands were visualized using Super ECL Detection Reagent (YEASEN, Shanghai, China).

2.4 Reverse Transcription-Quantitative Polymerase Chain Reaction

Total cellular RNA was isolated utilizing TRIzol reagent purchased from Life Technologies (Waltham, MA, USA). To eliminate genomic DNA contamination, the purified RNA underwent a 30-min digestion with RNase-free DNase I obtained from Promega (Madison, WI, USA). The HiScript III RT SuperMix for qPCR (+gDNA wiper) kit (Vazyme Biotech Co., Ltd., Nanjing, China) was used for reverse transcription of the DNase I-treated RNA. RT-qPCR was performed using the ChamQ Universal SYBR qPCR Master Mix (Vazyme Biotech Co., Ltd.) and a Bio-Rad CFX Connect detection system (Bio-Rad, Hercules, CA, USA). The following primer sequences were used: TMEM61: 5′-AGGGCTCGGGGGCAG-3′ (forward) and 5′-GCTCCCGTCACACATCTGG-3′ (reverse); GAPDH: 5′-ACCCACTCCTCCACCTT-3′ (forward) and 5′-CACCACCCTGTTGCTGTAG-3′ (reverse); PD-L1: 5′-AAATGGAACCTGGCGAAAG-3′ (forward) and 5′-GATGAGCCCCTCAGGCATTT-3′ (reverse).

2.5 Cell Proliferation Assay

The Cell Counting Kit-8 (APExBIO, Houston, TX, USA) was used to assess cell proliferation according to the manufacturer's instructions. Briefly, a 96-well plate was seeded with 2000 cells per well (Jet Biofil, Guangzhou, China). A BioTek microplate reader (Winooski, VT, USA) was used to measure absorbance at 450 nm.

2.6 Cell Migration and Invasion Assay

Transwell inserts containing membranes with 8-µm pores were placed in 24-well culture plates, with or without a Matrigel coating. A volume of 500 µL of complete culture medium supplemented with 10% FBS was loaded into the bottom compartments of Transwell plates to form a chemotactic gradient. After rinsing the cell pellets with Hanks' balanced salt solution (HBSS), SKOV3 and T29H cells were resuspended in serum-free culture medium and the cell suspension was plated onto the top inserts of Transwell devices. The plates were incubated for 24 h in a humidified incubator maintained at 37 °C with 5% CO_2. After incubation, non-migrated cells retained on the apical side of the porous membrane were gently wiped away

with sterile cotton swabs. Cells that successfully traversed through the membrane pores to the basal side were fixed in pure methanol over a 10-min period, stained with 0.01% crystal violet working solution, and photographed under a DMI3000 M inverted microscope (Leica Microsystems, Wetzlar, Germany).

2.7 Wound Healing Assay

The siRNA-transfected T29H and SKOV3 cells maintained in a medium containing 2% FBS were scratched using a 1-mL pipette tip. Images were obtained at 0 and 24 h post-scratch.

2.8 Comet Assay

The comet assay was performed as previously described [18]. Images were acquired using an integrated microscopic imaging system (BZ-X800E; KEYENCE, Shanghai, China) and analyzed using ImageJ (version 1.8.0; https://imagej.net/ij/).

2.9 Immunofluorescence

Cells were treated with 4% (w/v) paraformaldehyde and then incubated overnight at 4 °C with either anti-double-stranded DNA (anti-dsDNA) antibody (Sigma-Aldrich, St. Louis, MO, USA; Cat#MAB1293; 1:500) or anti-γ-H2AX antibody (Cell Signaling Technology, Danvers, MA, USA; Cat#2577; 1:500). Subsequently, the cells were incubated at 37 °C for 30 min with goat anti-mouse-Alexa Fluor™ 488 (Thermo Fisher Scientific; 1:1000; for dsDNA detection) or with goat anti-rabbit-Alexa Fluor™ 488 (Thermo Fisher Scientific; 1:500; for γ-H2AX detection). Cell nuclei were stained with 200 ng/mL DAPI (Sigma-Aldrich) for 5 min and visualized using a LEICA DMi8 confocal microscope (Leica Microsystems). The number of γ-H2AX foci per cell was counted. Cytosolic dsDNA was quantified as cytosolic fluorescence intensity per cell. Approximately 100 cells per experiment were analyzed using ImageJ software.

2.10 Transcriptomic Data Analysis of Ovarian Cancer and Normal Ovarian Tissues

The GEPIA2 web-based analytical tool (http://gepia2.cancer-pku.cn/#index) was used to evaluate transcriptomic data of 426 ovarian cancer tissues from The Cancer Genome Atlas (TCGA) database and 88 normal ovarian tissues from the Genotype-Tissue Expression (GTEx) database to identify differentially expressed genes (DEGs) between ovarian cancer and normal ovarian tissues. Pathway enrichment analysis of the DEGs was conducted using the Metascape webserver (http://metascape.org). Survival analysis was performed using the web-based Kaplan-Meier Plotter tool (https://kmplot.com/analysis/index.php?p=home). Under the selected ovarian cancer analysis settings, 655 patients with available TMEM61 expression and overall survival data were included and stratified into low-expression (n = 174) and high-expression (n = 481) groups.

2.11 HR and NHEJ Repair Efficiency Assays

Non-homologous end joining (NHEJ) and homologous recombination (HR) assays were performed as previously described [19,20]. SKOV3 cells were transfected with the pSceI-Hygro-EGFP plasmid (for the NHEJ assay) or the pDR-GFP plasmid (for the HR assay) using Lipofectamine 2000 and subsequently selected with either 500 μg/mL hygromycin B or 2 μg/mL puromycin, respectively, to generate stable SKOV3-I-SceI-Hygro-EGFP and SKOV3-DR-GFP clones. The stable SKOV3-I-SceI-Hygro-EGFP and SKOV3-DR-GFP clones were transfected with pCBASceI, and NHEJ and HR efficiencies were quantified by measuring the percentage of EGFP-positive cells at 48 h after transfection using a flow cytometer (Beckman, Brea, CA, USA). The gating strategy was applied as follows: the single-cell suspension was first gated on a forward scatter area (FSC-A) versus side scatter area (SSC-A) plot to exclude debris. Single cells were then selected via FSC-A versus forward scatter height (FSC-H) to exclude doublets. FITC-positive cells were selected to quantify the NHEJ and HR efficiencies.

2.12 Quantification and Statistical Analysis

All experimental data were processed using GraphPad Prism 10 (GraphPad Software Inc., San Diego, CA, USA). Statistical differences between two groups were assessed using Student's *t*-test. For panels containing more than two groups, Student's *t*-tests were used only for the indicated pre-specified pairwise comparisons, rather than for all possible comparisons among groups. Two-way analysis of variance (ANOVA) followed by Bonferroni post-hoc correction was applied to the proliferation experiment involving both treatment and time as independent factors. We defined $\alpha = 0.05$ as the critical significance threshold, with $p < 0.05$ deemed indicative of statistically significant intergroup variations.

3. Results

3.1 TMEM61 Is Scarcely Expressed in Normal Ovarian Tissues but Upregulated in Ovarian Cancer Tissues

Transcriptome data from 426 ovarian cancer cases and 88 normal ovarian tissues were analyzed to identify DEGs using GEPIA2 with the criteria $|\log_2(\text{fold change})| \geq 1.5$ and $p \leq 0.01$. Compared with normal ovarian tissues, 1510 genes were upregulated and 2736 genes were downregulated in ovarian cancer tissues. Functional analysis indicated that the upregulated genes were primarily enriched in cell cycle regulation, immune regulation, and cell adhesion (Fig. 1A). The downregulated genes were enriched in muscle structure development, heart development, and extracellular matrix organization (Fig. 1B). TMEM61 was among the significantly upregulated genes, with minimal expression in most normal ovarian tissues but elevated expression in ovarian cancer tissues (Fig. 1C). Kaplan–Meier analysis indicated that TMEM61 expression was not sig-

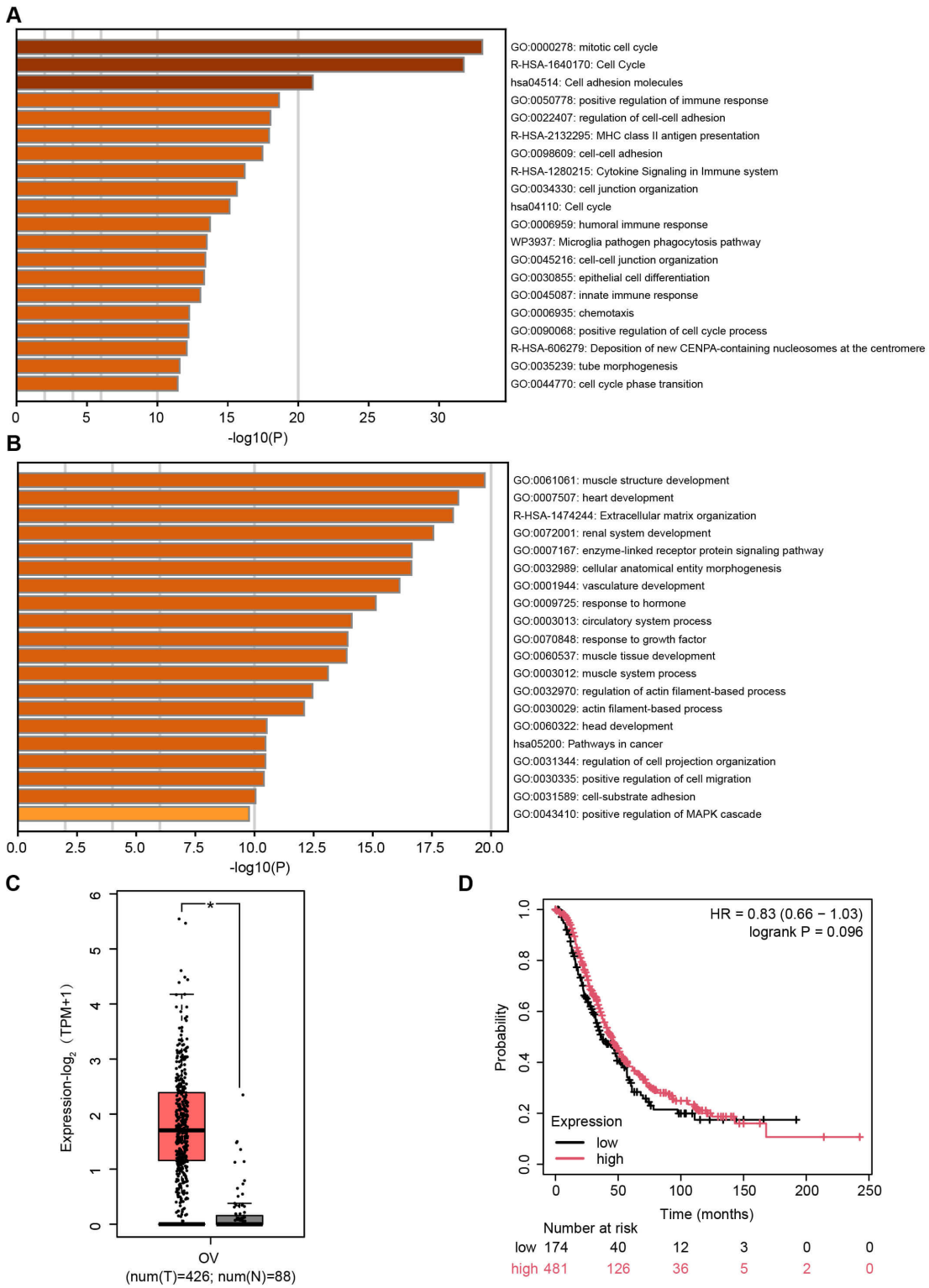

Fig. 1. TMEM61 is upregulated in ovarian cancer tissues. (A) Metascape pathway enrichment analysis of upregulated genes (log_2(fold change) ≥ 1.5, $p \leq 0.01$) in ovarian cancer tissues. (B) Metascape pathway enrichment analysis of downregulated genes (log_2(fold change) ≤ -1.5, $p \leq 0.01$) in ovarian cancer tissues. (C) TMEM61 expression levels in normal ovarian tissues and ovarian cancer tissues. (D) Correlation between TMEM61 expression in tumor tissues and overall survival of patients with ovarian cancer. *$p < 0.05$. OV, ovarian cancer; TMEM61, transmembrane protein 61; GO, gene ontology; R-HSA, Reactome-Homo sapiens; CENPA, centromere protein A; HR, hazard ratio.

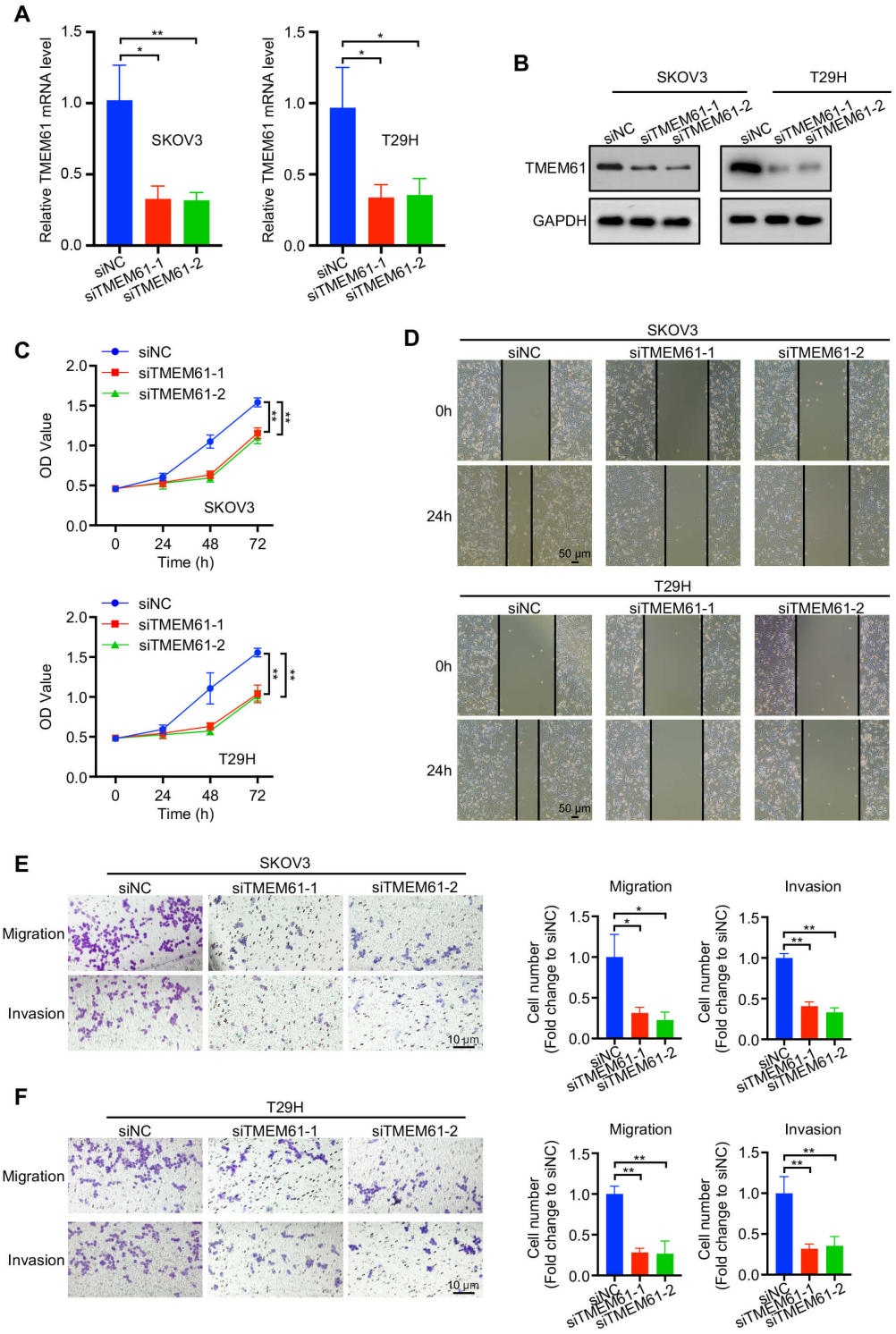

Fig. 2. TMEM61 knockdown inhibits ovarian cancer cell proliferation, migration, and invasion. (A,B) SKOV3 and T29H cells were transfected with control or TMEM61 siRNAs. Knockdown efficiency was evaluated after 48 h using RT-qPCR (A) and immunoblotting (B). (C) Cell proliferation following TMEM61 knockdown was measured using CCK-8 assays. (D) Wound healing assays were used to measure cell migration. Scale bar, 50 μm. (E,F) Cell migration and invasion were evaluated using Transwell assays. Scale bar, 10 μm. Data are expressed as the mean ± standard deviation of three biological replicates. *$p < 0.05$; **$p < 0.01$. Two-sided Student's *t*-tests were used for A, E, and F. Meanwhile, two-way analysis of variance was used for C. NC, negative control; RT-qPCR, reverse transcription-quantitative polymerase chain reaction; CCK-8, cell counting kit-8.

nificantly associated with overall survival in patients with ovarian cancer (log-rank $p = 0.096$; Fig. 1D). This suggests that TMEM61 expression alone may not be sufficient to stratify prognosis in the ovarian cancer survival dataset analyzed using Kaplan-Meier Plotter.

3.2 TMEM61 Knockdown Inhibits Ovarian Cancer Cell Proliferation, Migration, and Invasion

To investigate the function of TMEM61 in ovarian cancer cells, TMEM61 was knocked down in two ovarian cancer cell lines, and knockdown efficiency was confirmed via quantitative RT-qPCR and immunoblotting (Fig. 2A,B). CCK-8 assays demonstrated that TMEM61 knockdown inhibited ovarian cancer cell proliferation (Fig. 2C). Wound healing assays demonstrated that TMEM61 knockdown suppressed ovarian cancer cell migration (Fig. 2D), and Transwell assays demonstrated that TMEM61 knockdown inhibited ovarian cancer cell migration and invasion (Fig. 2E,F).

3.3 TMEM61 Knockdown Induces DNA Damage and Leads to Cytosolic DNA Accumulation in Ovarian Cancer Cells

DNA damage is a pivotal driver of tumor initiation and malignant progression [21,22]. On this basis, we examined whether TMEM61 participates in the regulation of DNA damage repair pathways. The comet assay results indicated that TMEM61 depletion induced robust DNA strand breaks (Fig. 3A). Immunofluorescence staining showed abundant phosphorylated H2AX (γ-H2AX) foci upon TMEM61 silencing (Fig. 3B). DNA damage triggers the leakage of nuclear DNA into the cytoplasmic compartment [23]. Our immunofluorescence analysis indicated that TMEM61 knockdown led to cytosolic DNA accumulation (Fig. 3C). Reporter assays indicated that loss of TMEM61 compromised DNA double-strand break (DSB) repair efficiency mediated by the HR and NHEJ pathways (Fig. 3D,E).

3.4 TMEM61 Knockdown Upregulates PD-L1 Expression in Ovarian Cancer Cells

Cytosolic DNA promotes PD-L1 expression by activating the cGAS-STING pathway [24]. Consistent with the finding that TMEM61 knockdown induced cytosolic DNA accumulation (Fig. 3C), we found that TMEM61 knockdown increased PD-L1 mRNA and protein expression (Fig. 4A,B). TREX1, a DNA exonuclease, inhibits cGAS-STING pathway activation by degrading cytosolic DNA [25]. We found that TREX1 overexpression reduced cytosolic DNA levels and suppressed the upregulation of PD-L1 induced by TMEM61 knockdown (Fig. 4C–E). Collectively, these findings indicate that TMEM61 knockdown induces PD-L1 expression by increasing cytosolic DNA levels.

4. Discussion

TMEM family members are implicated in the regulation of cell proliferation, migration, invasion, and epithelial–mesenchymal transition during malignant transformation and tumor progression [13,14,15]. Nevertheless, the oncogenic role of TMEM61, an uncharacterized member within this family, has yet to be fully elucidated. TMEM61 expression has been documented in clear cell renal cell carcinoma [26]. Here, we found that TMEM61 was barely detectable in the majority of normal ovarian specimens. Meanwhile, its expression was elevated in ovarian carcinoma tissues. Functional experiments showed that TMEM61 silencing strongly suppressed the proliferative, migratory, and invasive capacities of ovarian cancer cells. We also identified a hitherto undescribed function of TMEM61 in regulating DSB repair. TMEM61 depletion compromised DSB repair through both the HR and NHEJ pathways, thereby triggering DNA damage. TMEM61 knockdown drove PD-L1 upregulation by facilitating the cytoplasmic accumulation of dsDNA. Therefore, combinatorial blockade of TMEM61 and PD-L1 warrants further preclinical validation as a potential therapeutic modality for ovarian cancer.

Although TMEM61 is undetectable in most normal ovarian tissues, robust TMEM61 expression was detected in a small fraction of normal ovarian samples. Future work should examine the regulatory mechanisms underlying TMEM61 expression, determine the biological basis for its aberrant upregulation in this subset of normal ovarian tissues, and clarify whether these TMEM61-high ovarian tissues harbor precancerous lesions.

Overall, we have demonstrated that TMEM61 knockdown represses proliferation, migration, and invasion in ovarian cancer cells. However, the precise molecular mechanisms through which TMEM61 regulates these malignant behaviors remain undetermined. Moreover, in this study, all cellular functional assays were performed exclusively in SKOV3 and T29H cell lines, which cannot fully recapitulate the extensive molecular heterogeneity inherent to ovarian cancer. Further *in vivo* investigations using xenograft models and other orthotopic ovarian cancer animal models are warranted to further examine the biological functions of TMEM61. In addition, given that TMEM61 promotes DNA repair and that TMEM61 knockdown induces DNA damage, it would be worthwhile to further explore whether TMEM61 modulates the susceptibility of ovarian tumor cells to radiotherapy and chemotherapy and whether TMEM61 silencing can synergistically increase the sensitivity of cancer cells to these cytotoxic treatments. It is also warranted to elucidate the molecular mechanism underlying the regulation of DNA repair by TMEM61.

5. Limitations

Although our results have shown that TMEM61 facilitates proliferation, migration and invasion of ovarian can-

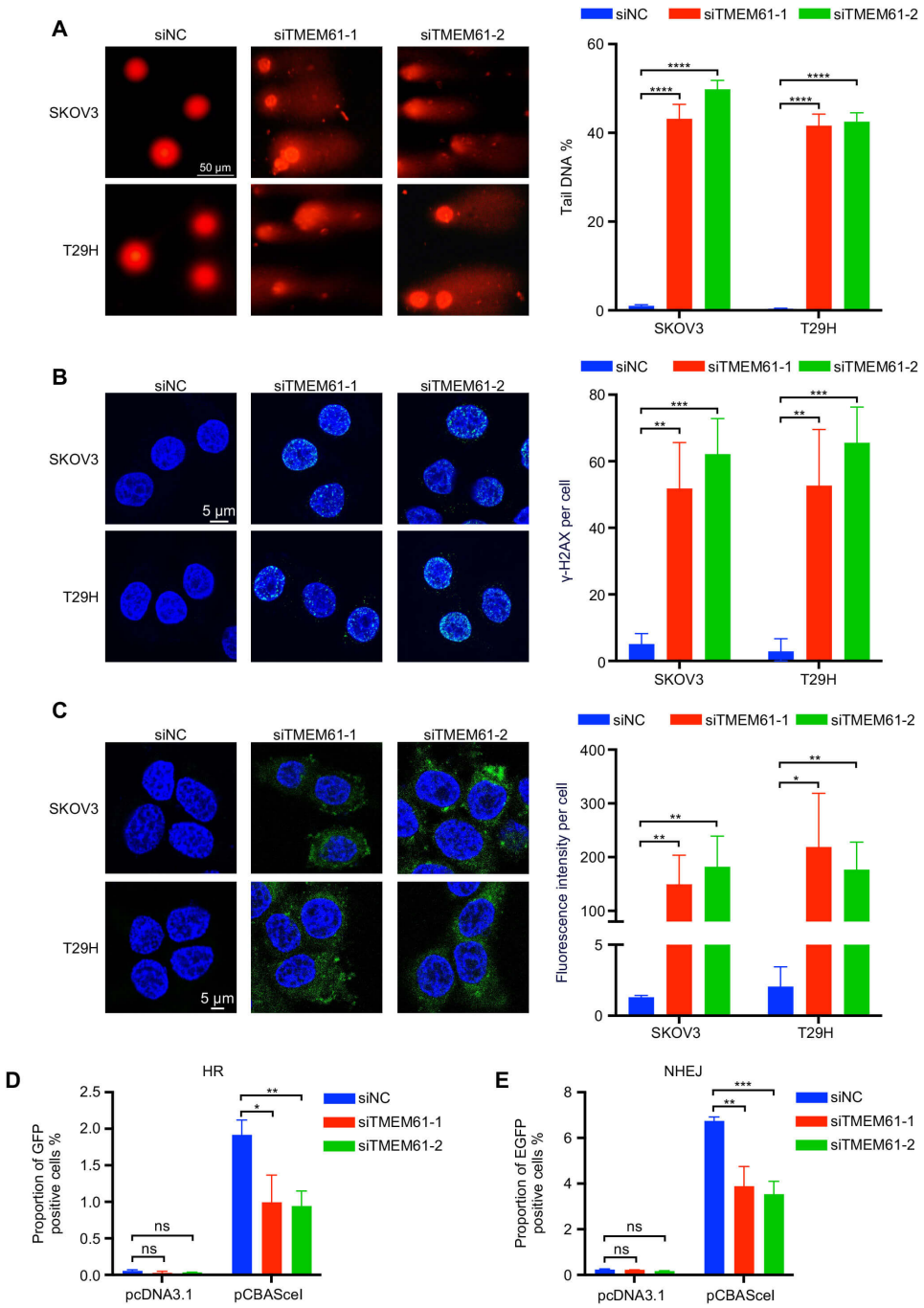

Fig. 3. TMEM61 knockdown induces DNA damage and leads to cytosolic DNA accumulation in ovarian cancer cells. (A–C) SKOV3 and T29H cells were transfected with control or TMEM61 siRNAs. DNA damage was assessed using a comet assay (A) and immunofluorescence of γ-H2AX foci (B); cytosolic double-stranded DNA levels were detected using anti-dsDNA (C) at 48 h after transfection. Scale bars: 50 μm in (A) and 5 μm in (B,C). (D,E) Control siRNAs and TMEM61 siRNAs were separately co-transfected with the control plasmid (pcDNA3.1) or the pCBASceI plasmid into SKOV3-DR-GFP cells (HR reporter assay, panel D) and SKOV3-I-SceI-Hygro-EGFP cells (NHEJ reporter assay, panel E). Forty-eight hours post-transfection, the fraction of GFP- or EGFP-positive cells was calculated. The number of γ-H2AX foci per cell was counted to quantify γ-H2AX staining signal, whereas cytosolic dsDNA was quantified by measuring cytosolic fluorescence intensity using ImageJ software. Approximately 100 cells were analyzed for each condition over three independent experiments in total. Data are expressed as the mean ± standard deviation of three biological replicates. *$p < 0.05$; **$p < 0.01$; ***$p < 0.001$; ****$p < 0.0001$; ns, not significant ($p > 0.05$). Two-sided Student's *t*-tests were used for (A–E). HR, homologous recombination; NC, negative control; NHEJ, non-homologous end joining; γ-H2AX, H2AX phosphorylation; anti-dsDNA, anti-double-stranded DNA; pCBASceI, pCBASceI plasmid; DR-GFP, pDR-GFP plasmid; EGFP, enhanced green fluorescent protein.

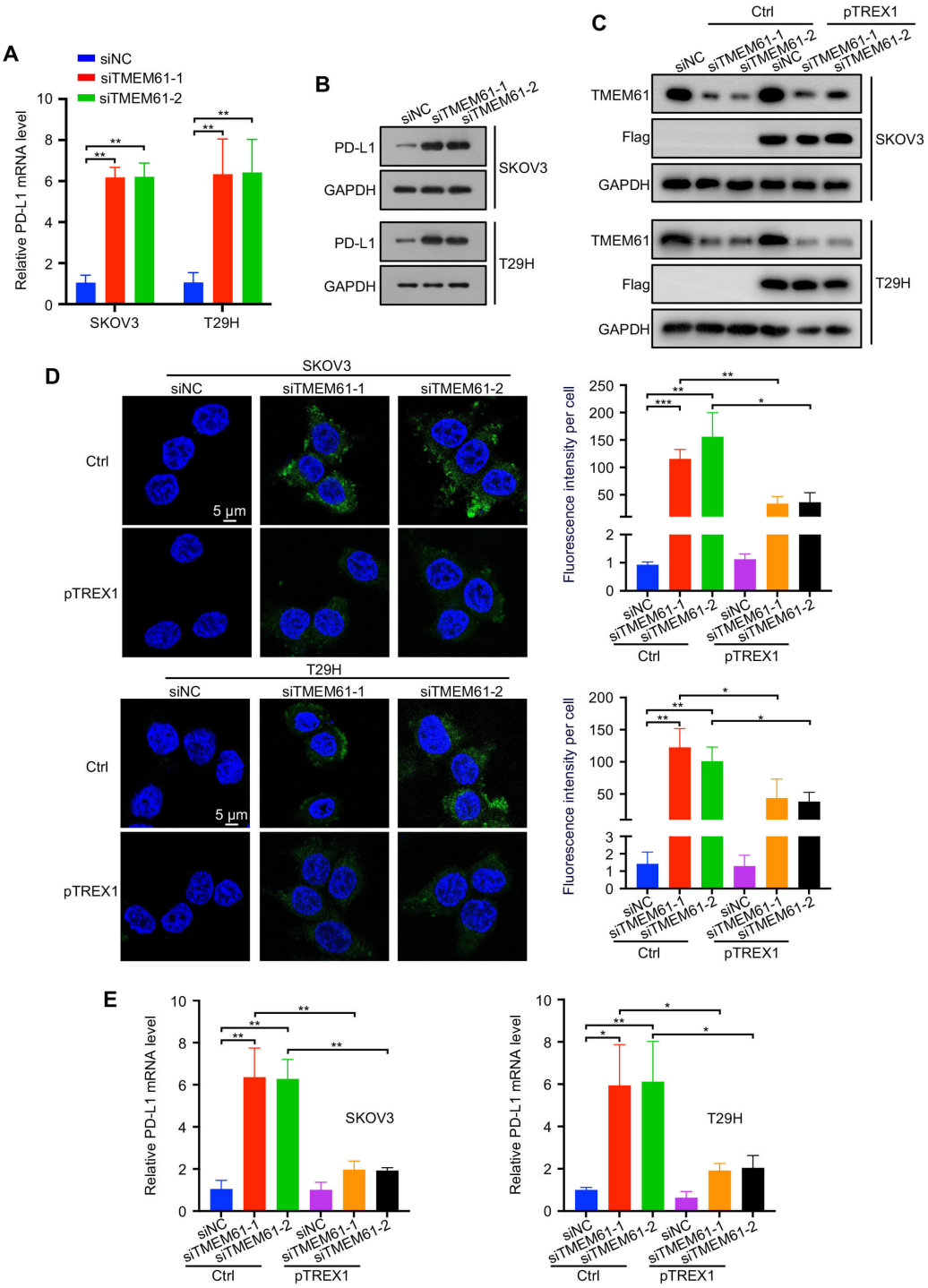

Fig. 4. TMEM61 knockdown increases PD-L1 expression in ovarian cancer cells. (A,B) SKOV3 and T29H cells were transfected with control or TMEM61 siRNAs; the mRNA (A) and protein (B) levels of PD-L1 were measured using RT-qPCR and immunoblotting, respectively, at 48 h after transfection. (C–E) SKOV3 and T29H cells were co-transfected with the control or TMEM61 siRNAs and either a Flag-TREX1 expression plasmid or a control plasmid. TMEM61 and Flag-TREX1 protein levels were assessed using immunoblotting (C), cytosolic double-stranded DNA levels were detected via immunofluorescence (D), and PD-L1 expression levels were measured using RT-qPCR (E) at 48 h after transfection. Scale bar, 5 μm. Data are expressed as the mean ± standard deviation of three biological replicates. Cytosolic dsDNA was quantified via ImageJ software, with approximately 100 individual cells assessed per experimental group throughout three independent biological replicates. *$p < 0.05$; **$p < 0.01$; ***$p < 0.001$. Two-sided Student's t-tests were used for A, D, and E. Ctrl, control; NC, negative control; PD-L1, programmed death-ligand 1; TREX1, three prime repair exonuclease 1.

cer cells and strengthens DNA damage repair capacity, the precise molecular mechanisms underlying these oncogenic and genome-protective functions remain unclear. All functional experiments were performed exclusively in *in vitro*-cultured SKOV3 and T29H cell lines, which cannot fully recapitulate the extensive molecular heterogeneity inherent to ovarian cancer.

6. Conclusions

In summary, the present study reveals TMEM61 as a previously uncharacterized oncogenic driver that facilitates malignant progression of ovarian cancer. Loss of TMEM61 triggers robust DNA double-strand breaks and cytoplasmic dsDNA buildup, thus increasing the expression of the immune checkpoint molecule PD-L1. Collectively, these results highlight TMEM61 as a promising diagnostic biomarker and druggable therapeutic candidate for ovarian cancer.

Availability of Data and Materials

The datasets generated and analyzed during the current study are available from the corresponding author upon reasonable request.

Author Contributions

All authors contributed to the study conception and design. KFT conceived and designed the study. ZZD and RLT performed the experiments and analyzed the data. ZZD drafted the manuscript. KFT reviewed the manuscript. KFT supervised the study. All authors contributed to editorial changes in the manuscript. All authors read and approved the final manuscript. All authors have participated sufficiently in the work and agreed to be accountable for all aspects of the work.

Ethics Approval and Consent to Participate

Not applicable. This study used only established cell lines and did not involve human participants or animals.

Acknowledgment

The authors wish to thank Editage for English language editing.

Funding

This work was supported by the Chongqing Medical University Program for Youth Innovation in Future Medicine (grant number W0084).

Conflicts of Interest

The authors declare no conflicts of interest. Given his role as an Editorial Board member, Kai-Fu Tang had no involvement in the peer-review of this article and has no access to information regarding its peer review. Full responsibility for the editorial process for this article was delegated to Sung Eun Kim.

Declaration of AI and AI-Assisted Technologies in the Writing Process

During the preparation of this work, the authors used Doubao, Gemini 3.1 Pro and ChatGPT 5.6 to check spelling and grammar. The authors reviewed and edited the content as needed and take full responsibility for the content of the publication.

References

[1] Konstantinopoulos PA, Matulonis UA. Clinical and translational advances in ovarian cancer therapy. Nature Cancer. 2023; 4: 1239–1257. https://doi.org/10.1038/s43018-023-00617-9

[2] Siegel RL, Kratzer TB, Wagle NS, Sung H, Jemal A. Cancer statistics, 2026. CA: a Cancer Journal for Clinicians. 2026; 76: e70043. https://doi.org/10.3322/caac.70043

[3] Kuroki L, Guntupalli SR. Treatment of epithelial ovarian cancer. BMJ (Clinical Research Ed.). 2020; 371: m3773. https://doi.org/10.1136/bmj.m3773

[4] Kandalaft LE, Dangaj Laniti D, Coukos G. Immunobiology of high-grade serous ovarian cancer: lessons for clinical translation. Nature Reviews. Cancer. 2022; 22: 640–656. https://doi.org/10.1038/s41568-022-00503-z

[5] Kandalaft LE, Odunsi K, Coukos G. Immunotherapy in Ovarian Cancer: Are We There Yet? Journal of Clinical Oncology: Official Journal of the American Society of Clinical Oncology. 2019; 37: 2460–2471. https://doi.org/10.1200/JCO.19.00508

[6] Lheureux S, Braunstein M, Oza AM. Epithelial ovarian cancer: Evolution of management in the era of precision medicine. CA: a Cancer Journal for Clinicians. 2019; 69: 280–304. https://doi.org/10.3322/caac.21559

[7] Zhu Y, Song J, Zhu Y, Xu H, Lang S, Yang X, et al. Emerging Biomaterials Blocking PD-1/PD-L1 Pathway for Cancer Therapy. Advanced Materials (Deerfield Beach, Fla.). 2026; 38: e17019. https://doi.org/10.1002/adma.202517019

[8] Ghisoni E, Morotti M, Sarivalasis A, Grimm AJ, Kandalaft L, Laniti DD, et al. Immunotherapy for ovarian cancer: towards a tailored immunophenotype-based approach. Nature Reviews. Clinical Oncology. 2024; 21: 801–817. https://doi.org/10.1038/s41571-024-00937-4

[9] Zheng Y, Yang F, Wang M, Wang Z, Zhang X, Huo C, et al. Ceramide disrupts TM9SF2-PGK1 axis to redirect PD-L1 trafficking and enhance antitumor immunity. Nature Communications. 2026; 17: 4525. https://doi.org/10.1038/s41467-026-70764-x

[10] Iwai Y, Ishida M, Tanaka Y, Okazaki T, Honjo T, Minato N. Involvement of PD-L1 on tumor cells in the escape from host immune system and tumor immunotherapy by PD-L1 blockade. Proceedings of the National Academy of Sciences of the United States of America. 2002; 99: 12293–12297. https://doi.org/10.1073/pnas.192461099

[11] Mirza MR, Coleman RL, González-Martín A, Moore KN, Colombo N, Ray-Coquard I, et al. The forefront of ovarian cancer therapy: update on PARP inhibitors. Annals of Oncology: Official Journal of the European Society for Medical Oncology. 2020; 31: 1148–1159. https://doi.org/10.1016/j.annonc.2020.06.004

[12] Guerra C, Kalaitsidou M, Kueberuwa G, Hawkins R, Edmondson R. Engineering strategies to optimise adoptive cell therapy in ovarian cancer. Cancer Treatment Reviews. 2023; 121: 102632. https://doi.org/10.1016/j.ctrv.2023.102632

[13] Marx S, Dal Maso T, Chen JW, Bury M, Wouters J, Michiels C, et al. Transmembrane (TMEM) protein family members: Poorly characterized even if essential for the metastatic process. Seminars in Cancer Biology. 2020; 60: 96–106. https://doi.org/10.1016/j.semcancer.2019.08.018

[14] Schmit K, Michiels C. TMEM Proteins in Cancer: A Review. Frontiers in Pharmacology. 2018; 9: 1345. https://doi.org/10.3389/fphar.2018.01345
[15] Zhang N, Pan H, Liang X, Xie J, Han W. The roles of transmembrane family proteins in the regulation of store-operated Ca2+ entry. Cellular and Molecular Life Sciences: CMLS. 2022; 79: 118. https://doi.org/10.1007/s00018-021-04034-y
[16] Wang S, Zhou Q, Yan S, Liu C, Li F, Feng D, et al. TMEM17 Promotes Tumor Progression in Glioblastoma by Activating the PI3K/AKT Pathway. Frontiers in Bioscience (Landmark Edition). 2024; 29: 285. https://doi.org/10.31083/j.fbl2908285
[17] Yang G, Rosen DG, Liu G, Yang F, Guo X, Xiao X, et al. CXCR2 promotes ovarian cancer growth through dysregulated cell cycle, diminished apoptosis, and enhanced angiogenesis. Clinical Cancer Research: an Official Journal of the American Association for Cancer Research. 2010; 16: 3875–3886. https://doi.org/10.1158/1078-0432.CCR-10-0483
[18] Luo YW, Zhou JP, Ji H, Xu D, Zheng A, Wang X, et al. SARS-CoV-2 N protein-induced Dicer, XPO5, SRSF3, and hnRNPA3 downregulation causes pneumonia. Nature Communications. 2024; 15: 6964. https://doi.org/10.1038/s41467-024-51192-1
[19] Chen X, Li WF, Wu X, Zhang HC, Chen L, Zhang PY, et al. Dicer regulates non-homologous end joining and is associated with chemosensitivity in colon cancer patients. Carcinogenesis. 2017; 38: 873–882. https://doi.org/10.1093/carcin/bgx059
[20] Pierce AJ, Johnson RD, Thompson LH, Jasin M. XRCC3 promotes homology-directed repair of DNA damage in mammalian cells. Genes & Development. 1999; 13: 2633–2638. https://doi.org/10.1101/gad.13.20.2633
[21] Kotsantis P, Petermann E, Boulton SJ. Mechanisms of Oncogene-Induced Replication Stress: Jigsaw Falling into Place. Cancer Discovery. 2018; 8: 537–555. https://doi.org/10.1158/2159-8290.CD-17-1461
[22] Groelly FJ, Fawkes M, Dagg RA, Blackford AN, Tarsounas M. Targeting DNA damage response pathways in cancer. Nature Reviews. Cancer. 2023; 23: 78–94. https://doi.org/10.1038/s41568-022-00535-5
[23] Suptela AJ, Marriott I. Cytosolic DNA sensors and glial responses to endogenous DNA. Frontiers in Immunology. 2023; 14: 1130172. https://doi.org/10.3389/fimmu.2023.1130172
[24] Cheng AN, Cheng LC, Kuo CL, Lo YK, Chou HY, Chen CH, et al. Mitochondrial Lon-induced mtDNA leakage contributes to PD-L1-mediated immunoescape via STING-IFN signaling and extracellular vesicles. Journal for Immunotherapy of Cancer. 2020; 8: e001372. https://doi.org/10.1136/jitc-2020-001372
[25] Wang Q, Du J, Hua S, Zhao K. TREX1 plays multiple roles in human diseases. Cellular Immunology. 2022; 375: 104527. https://doi.org/10.1016/j.cellimm.2022.104527
[26] Wrzesiński T, Szelag M, Cieślikowski WA, Ida A, Giles R, Zodro E, et al. Expression of pre-selected TMEMs with predicted ER localization as potential classifiers of ccRCC tumors. BMC Cancer. 2015; 15: 518. https://doi.org/10.1186/s12885-015-1530-4